6th IEEE RAS/EMBS International Conference on
Biomedical Robotics and Biomechatronics (BioRob)
June 26-29, 2016. UTown, Singapore

Coupled Systems Analyses for High-performance Robust Force Control of Wearable Robots

Thiago Boaventura, Jonas Buchli

***Abstract*— A wearable robot is constantly in contact with its user. To properly and safely perform tasks together with the wearer, such as walking and load carrying, it is important that the robot is able to control its joint torques. To enhance the performance of torque/force controllers, feedforward controllers such as velocity and friction compensation are commonly used. Although such controllers are able to enhance the torque closed-loop bandwidth, they can also significantly reduce the system's robustness. For coupled systems, such as wearable robots, the soft human skin and the compliance of the human/robot attachment pose additional challenges to the performance and stability of such controllers. In this paper we investigate the robustness issues associated with the force control on coupled systems, performing thorough analyses of the torque loop sensitivity, including how the attachment stiffness and the human impedance may influence it. Based on these analyses, we propose two potential control solutions that may improve both the disturbance attenuation and torque reference tracking on wearable robots.**

I. Introduction

Robots are often in contact with the environment, people, or other objects. Wearable robots, such as exoskeletons and limb-prostheses, are in addition inherently coupled to a wearer. This close attachment allows the robot to symbiotically move with the user, providing e.g. physical assistance or power augmentation. In these and other typical applications of wearable robots, it is desirable to control the forces/torques the robot applies to the user and to the environment. Such robot force control capabilities allow an easy implementation of advanced control methods such as impedance [1] and admittance control [2], operational space control [3], inverse dynamics control, virtual model control [4], as well as the control of the contact and interaction forces. Note that throughout this paper the terms *force* and *torque* are used interchangeably.

Joint force control is clearly an important and advantageous feature for wearable robots. To enhance the performance of such force controllers, control designers commonly make use of feedforward controllers, such as viscous friction compensation [5]. Another important phenomenon in the force dynamics, which can also be compensated for through model-based feedforward control, consists of an intrinsic load velocity feedback present in the open-loop force dynamics [6] no matter what kind of actuation system is employed [7]. Because of this natural load velocity feedback, the open and closed-loop robot force dynamics may be strongly limited by the characteristics (e.g. stiffness, inertia, damping) of the load driven by the robot actuators. For wearable robots, in particular, besides the robot links, the human is also part of the load seen by the robot. Therefore, the characteristics of the human as well as of the human/robot attachment impose additional challenges in the robot force control.

Coupled systems, in general, have a coupling stiffness that is usually orders of magnitude more compliant than the rest of the mechanical structures. In wearable robots, this soft attachment consists normally of elastic bands that connect the human limbs to the robot links. In addition, human soft tissues make such human/robot coupling even more compliant [8]. In terms of force control, this soft coupling element causes a phase drop into the open-loop force dynamics at low frequencies [9], reducing the system robustness at frequencies which are usually of interest for locomotion and manipulation. In this paper we will use a simple abstraction of a coupled system to illustrate the human/robot interaction dynamics on wearable robots. The main contributions of this work can be summarized as follows: 1) A sensitivity-based analysis of the robustness of closed-loop force controllers on coupled systems with feedforward control; and 2) Proposition of two potential control designs to enhance the system robustness: a notch filter and a lead compensator.

Last but bot least, it is important to highlight that although the focus of this paper is on wearable robots, the issues presented and discussed in here may be relevant to broader areas of robotics in which the robot is *not* physically attached to a user. This includes the control of robots with mechanical compliance, such as series elastic actuators [10], [11]; and the control of robots that are in constant interaction with unknown environments, like legged robots, which have their feet temporarily coupled to the ground every time they are in stance.

II. Modelling

In this section we will derive two conceptual models with 1 Degree Of Freedom (DOF) which are simple enough to use intuition, and yet include the limitations caused by the human/robot attachment into the robot force control. The first model will describe the force dynamics in robots that are *not* attached to a human, called throughout this paper *ordinary robots*. The second model will illustrate a *wearable robot*, in which a human is attached to the system.

A. Ordinary robots

Force is always generated over an element that is deformable or compressible, i.e. an impedance. Impedances (e.g. springs), by definition, have velocity as input to their

T.Boaventura and J. Buchli are with the Agile and Dexterous Robotics Lab, ETH Zürich. tboventura@ethz.ch, buchlij@ethz.ch

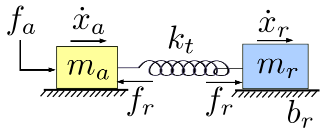

Fig. 1: The actuator inertia m_a is accelerated by an external force, and its velocity is transmitted to a compliant transmission, with stiffness k_t, which connects the actuator to the robot link with inertia m_r and damping b_r. In case there is a relative motion between actuator and robot link, a force is generated at the transmission.

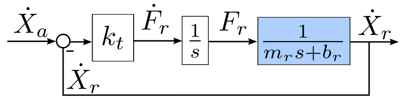

Fig. 2: Block diagram for a generic actuator acting on a robotic link through a transmission stiffness. The robot velocity $\dot{X}_r(s)$ is clearly being fed back into the robot force dynamics. This is the open-loop dynamics, i.e. there is no controller depicted in the diagram.

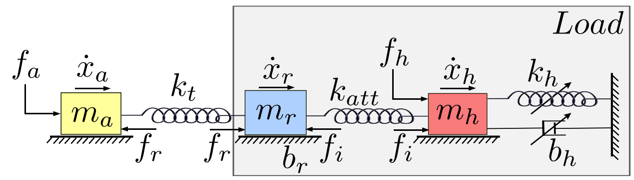

Fig. 3: Wearable robot schematics with a human block (in red), with mass m_h, and variable stiffness k_h and damping b_h. The human/robot attachment is depicted as a pure spring with stiffness k_{att}. A compression/extension on the attachment will produce an interaction force f_i.

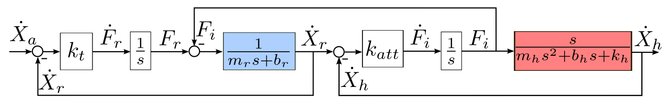

Fig. 4: Block diagram for a generic actuator acting on a wearable robot link (in blue), which is attached to a human (in red). The interaction force $F_i(s)$, through a feedback, couples robot and human dynamics.

dynamics and force as output. Admittances (e.g. masses, inertias), on the other hand, have the opposite input/output relation, that is, forces as input and velocity as output. Therefore, because of causality reasons, an inertia should always be connected to another inertia through a spring [1].

By applying such concepts to robots, we can say the joints of a robot are driven by an actuation system composed of an inertia and a compliant transmission. In one hand, the actuator inertia m_a (e.g. a rotor in an electric motor) moves and transmits a velocity $\dot{x}_a$ to the transmission, In other words, the actuator inertia can be seen as a *velocity source* to the transmission stiffness. This actuator inertia is accelerated by an external force f_a (e.g. electromagnetic forces generated by the stator). On the other hand, the transmission is the most compliant element which connects the actuator inertia (i.e. rotor) to the load inertia m_r (e.g. the robot link inertia). This transmission, generally few orders of magnitude more compliant than the actuator inertia, converts the inertia velocity into a force, which is then applied to both actuator and load inertias. An example of transmission could be a gearbox or a harmonic gear that connects the rotor of a motor to the link of the robot. Series elastic actuators have a spring as transmission, which is also used to measure the transmission force f_r in most of the cases. Although we assume in here the transmission to be a pure spring, it could include also damping without loss of generality. This conceptual case is illustrated in Fig. 1.

$$\dot{f}_r = k_t \left(\dot{x}_a - \dot{x}_r\right) \tag{1}$$

The dynamics of the force transmitted from the actuator to the load is defined by Eq. 1. As we can see, this dynamics is characterised not only by the transmission stiffness k_t and the actuator dynamics, which determines how quickly $\dot{x}_a$ can be changed, but also by the robot rigid body dynamics through $\dot{x}_r$. This interaction between transmission force and load velocity is intrinsic to the physics, no matter the actuation technology and load characteristics, and it can be mathematically seen as a *load velocity feedback* [12]. Equation 1 can be expressed by the following transfer function:

$$\frac{F_r(s)}{\dot{X}_a(s)} = \frac{k_t\left(m_r s + b_r\right)}{s\left(m_r s + b_r\right) + k_t} \tag{2}$$

where $F_r(s)$ and $\dot{X}_a(s)$ are the Laplace transforms of f_r and $\dot{x}_a$, respectively.

An important consequence of the load velocity feedback into the force dynamics is the presence of a *load dependent zero*, as it can be seen in Eq. 2. This zero, usually located at low frequencies since the load damping b_r is kept as low as possible in real applications, may severely limit the force control performance [7].

B. Wearable robots

Wearable robots are intrinsically attached to a user through some compliant element, e.g. an elastic band fixed by Velcro®. From the robot actuator perspective, the load characteristics completely change by attaching a human to the robot links. Besides the human/robot attachment dynamics, the human may apply forces using a large range of joint impedances during tasks such as walking for instance [13], [14], [15].

The dynamics of such coupled system can be represented by the block diagram shown in Fig. 4. This block diagram shows that the robot and human dynamics are in series, and the interaction force $F_i(s)$ that couples both systems is also fed back in the diagram. In this case, the transfer function $F_r(s)/\dot{X}_a(s)$ has numerator of order 4 and denominator of order 5. Considering an additional second order dynamics with gain 1 for the actuator velocity:

$$\frac{\dot{X}_a(s)}{U_a(s)} = \frac{\omega_a^2}{s^2 + 2\xi_a\omega_a s + \omega_a^2} \tag{3}$$

where $U_a(s)$ is the actuator input (e.g. a voltage), ω_a the natural frequency, and ξ_a the damping, the denominator becomes of order 7. Since its symbolic expression does not provide meaningful insights, we are not going to show it in here. Instead, we will perform a numeral analysis using, for instance, $m_r = 5$, $b_r = 50$, $m_h = 10$, $b_h = 20$, $k_h = 100$,

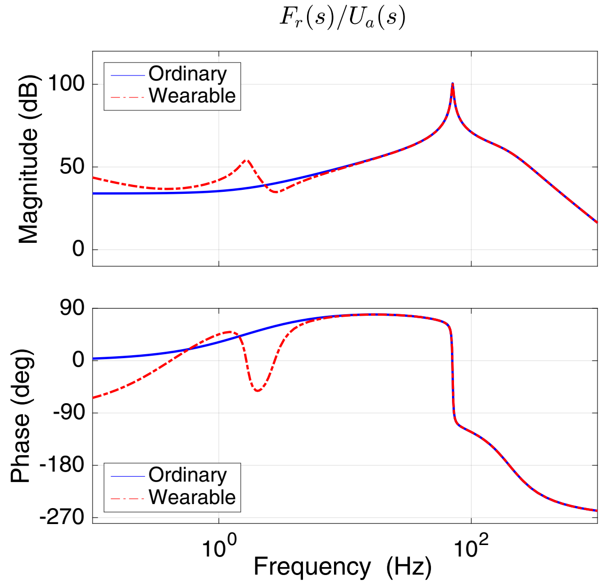

Fig. 5: Bode plot of the open-loop transfer function $F_r(s)/U_a(s)$ for ordinary (solid blue line) and a wearable (dash-dot red line) robot. The coupling with the human dynamics causes a resonance followed by an antiresonance at low frequencies. It also produces a large phase drop at the same frequencies. Such features are the most relevant differences in terms of force dynamics between an ordinary and a wearable robot.

$k_t = 10^6$, $k_{att} = 10^3$, $\omega_a = 1250$, and $\xi_a = 0.5$, all in SI units.

The frequency response of the open-loop transfer function $F_r(s)/U_a(s)$, shown in Fig. 5, illustrates the core difference between an ordinary robot, which is not attached to a user, and a wearable robot, which is intrinsically coupled with the user: *a phase drop at low frequencies*. Such drop in phase is caused by a resonance/antiresonance pair introduced by the soft human/robot attachment. As we will show next, such phase drop in the force dynamics increases the sensitivity of the closed-loop system at these low frequencies, possibly making the system unstable in practice. Also, generally such low frequencies are in the range of most of the common human tasks, such as walking and running.

The integrator present in the wearable robot force dynamics is due to the human stiffness k_h. This means that the robot force f_r raises linearly when the robot pushes the human away from its reference position. Furthermore, the high frequency resonance, common to both ordinary and wearable robots, is a result of the transmission dynamics. It is usually located in frequencies above those of interest in common applications, not posing big issues on the closed-loop performance and stability. The frequency of this resonance is mainly related to the transmission stiffness k_t and the robot mass m_r. At even higher frequencies, around 200 Hz in this case, we can also notice the dynamics of the actuator, which consists of 2 complex conjugated poles.

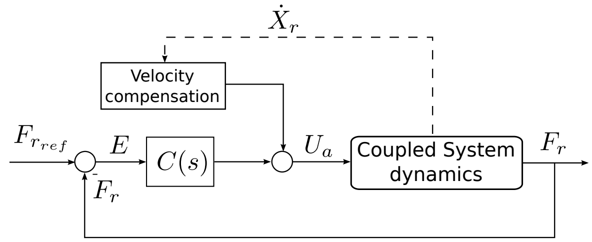

Fig. 6: Block diagram for the closed loop robot force control. It uses a feedback controller $C(s)$ and a feedforward velocity compensation controller. The coupled system dynamics is influenced by both the robot, human, and attachment dynamics.

III. Control

As seen in the previous section, the human/robot coupling considerably changes the load characteristics and consequently the open-loop dynamics of the force that is delivered by the actuator. In this section, we will close the robot force loop and investigate possible impacts of such coupling on the closed-loop performance and robustness.

A. Velocity compensation feedforward command

To achieve good fast convergence times and good closed-loop force tracking responses, it is paramount to compensate for the natural velocity feedback present in the force dynamics [7], [16], [17]. An intuitive way for compensating this load velocity influence is to measure it and to *continuously* provide, with our actuator, an extra velocity $\dot{x}_{ex} = \dot{x}_r$. In this case, the robot force dynamics would be given only by $\dot{f}_r = k_t((\dot{x}_a + \dot{x}_{ex}) - \dot{x}_r) = k_t\dot{x}_a$. Such feedforward compensation notably increases the closed-loop force bandwidth, as we can see in step responses shown in Fig. 7. Such velocity compensation has been successfully used in high-performance torque-controlled robots [18], [19]. A block diagram depicting the use of such controller is shown in Fig. 6.

Although it is possible to achieve better tracking performances with the velocity compensation feedforward control, its practical use in coupled systems as illustrated in Fig. 3 has been proven challenging. Differently than the uncoupled situation of ordinary robots, the system tends to become unstable at low frequencies when perturbed. Therefore, in the next section we present the sensitivity function of the closed-loop when using such compensation.

B. Sensitivity function

The sensitivity transfer function is the closed-loop transfer function that maps both the disturbances $D(s)$ to the robot force $F_r(s)$, and the force reference $F_{r_{ref}}(s)$ to the tracking error $E(s) = F_{r_{ref}}(s) - F_r(s)$, that is:

$$S(s) = \frac{1}{1 + L(s)} = \frac{F_r(s)}{D(s)} = \frac{E(s)}{F_{r_{ref}}(s)} \tag{4}$$

where $L(s) = C(s)\left({F_r(s)}/{U_a(s)}\right)$ is the Loop gain, being $C(s)$ the transfer function of the controller.

Ideally $S(s)$ should be low at the frequencies of interest, meaning disturbances would be attenuated and tracking error

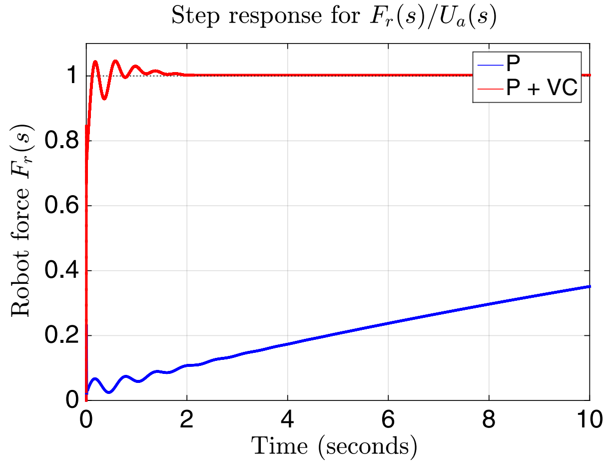

Fig. 7: Step response for the closed-loop robot force transfer function $F_r(s)/U_a(s)$ for the wearable robot case. A simple feedback P controller, in blue, was tuned to $K_p = 4.57 \cdot 10^{-4}$ to give phase margin $\phi_m = 45$ deg. When the feedforward velocity compensation (VC) is used, the system significantly increases its raising time while keeping the desired phase margin.

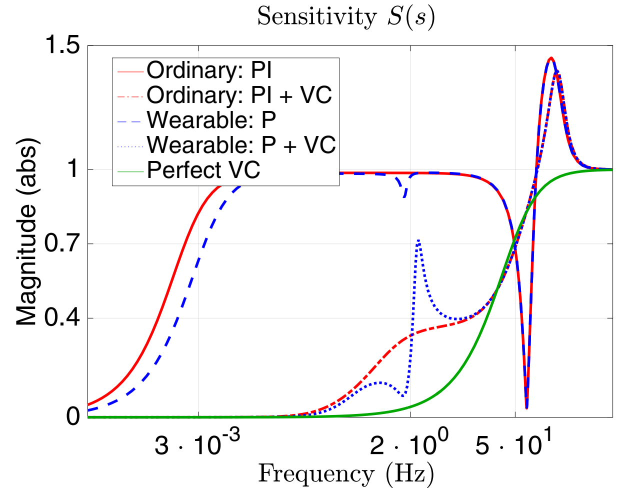

Fig. 8: Magnitude of the sensitivity function $S(s)$ for both ordinary (red) and wearable (blue) robots with different controllers. As we can see, the velocity compensation (VC) feedforward command remarkably increases the bandwidth for both systems. However, for wearable (coupled) systems, the VC critically affects the sensitivity around the human/robot attachment natural frequency, which is about 2 Hz in this case. The VC also pushes the sensitivity above 1 at high frequencies, with a peak at the natural frequency of the actuator dynamics, which is 200 Hz in this example. However, if the actuator dynamics is hypothetically neglected, a perfect velocity compensation would be achieved, and then the sensitivity would be smooth and with no peaks, as shown in green.

would be small at such frequencies, and high at higher frequencies to attenuate measurement noise [20], [21]. Furthermore, the peak of the sensitivity function $S(s)$ is also directly related to the stability properties of the system, including the phase and gain margins [22]. For instance, a peak $M_s = \max_{\omega} |S(j\omega)| = 1.5$ is approximately equivalent to a phase margin $\phi_m \geq 40$ deg. The larger the sensitivity peak, the closer to instability. Also, the sensitivity peak tends to be a more reliable indicator of relative stability than the gain and phase margin. It is possible to find situations where the gain and phase margin seem adequate, when actually a large sensitivity peak informs us of a very critical stability condition [23].

To asses the impact of the velocity compensation in both coupled and uncoupled systems, we performed a sensitivity analysis using both standard feedback controller with and without the velocity compensation. For the coupled case a simple P feedback controller was used, since the plant already has an integrator. For the uncoupled case, a PI was used in order to have comparable closed-loop plants. The results depicted in Fig. 8 highlight two important characteristics: *a)* both velocity-compensated systems increase their bandwidth, i.e. the frequency where their magnitude crosses 0.708 $(-3\ dB)$, in about 4 orders of magnitude; and *b)* the velocity-compensated sensitivity for the wearable robot system has a dent around the human/robot attachment natural frequency. This latest characteristic means the system, at that frequency, will be less robust to disturbances and system variations, and the closed-loop tracking response will be worse. Such findings do match our empirical experience in force control of coupled systems. In addition, Fig. 8 also shows that in case a perfect velocity compensation could be achieved, by hypothetically having infinitely fast actuators and a perfect model, both coupled and uncoupled systems would have an ideal and smooth sensitivity function.

In order to get additional insights on how some of the parameters influence the force dynamics sensitivity, we performed further analyses by varying these parameters in a specific range. As shown in Fig. 9, variations on the attachment stiffness k_{att} are the most critical ones in terms of robustness. More specifically, the more rigid the attachment the higher the sensitivity at the attachment natural frequency.

In the next sections we will propose two different but possibly complementary control solutions to improve the robustness of the force controller in low-frequencies.

C. Notch filter

The dent, or notch, caused by the velocity compensation feedforward controller on the sensitivity function of the wearable robot case is an undesirable side effect, as previously discussed. Such feature is caused by the resonance/antiresonance pair introduced by the human/robot attachment on the system magnitude, which leads to a phase drop. The shape of such characteristic connotes the use of a *notch filter*, which would be able to add some phase at that particular frequency, minimally affecting other parts of the plant frequency spectrum [22], [20].

The notch filter should be added around the frequencies of the attachment stiffness, aiming at minimizing its effects at that frequency. In our case, we used a filter with complex zeros, to attract the lightly-damped low frequency poles, and two identical real poles:

$$G_{notch} = \frac{0.01s^2 + 0.04s + 1}{(s+13)^2} \tag{5}$$

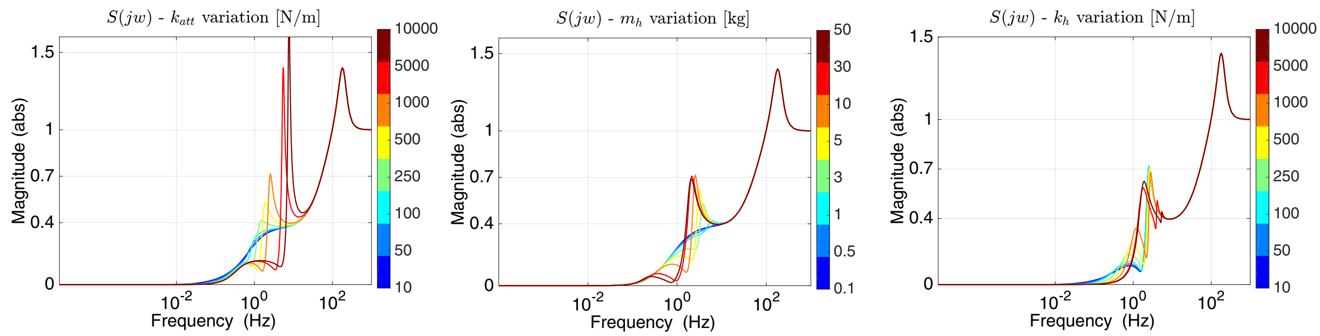

(a) $k_{att} \in \left[10, 10^4\right]$ N/m.

(b) $m_h \in [0.1, 50]$ kg

(c) $k_h \in \left[10, 10^4\right]$ N/m

Fig. 9: Sensitivity function $S(s)$ for coupled systems using velocity compensation for different parameters. As we can see, rigid human/robot attachments k_{att} tend to dangerously increase the system sensitivity at low frequencies. Variations on the human inertia m_h and stiffness k_h also affect the system, but in lower scales. For instance, the lighter the human (link) mass, the more attenuated the sensitivity dent at the attachment natural frequency. Changes in the human stiffness k_h did not attenuate the middle sensitivity peak, but instead they changed its shape.

The result of applying such filter in series with the feedback and velocity feedforward controllers is shown in dashed black in Fig. 10. As we can see, the notch filter manages to reduce the sensitivity at the attachment resonance frequency, making it even lower than for the uncoupled system. However, due to the unavoidable waterbed effect [24], by pushing the sensitivity down at the attachment frequency, the peak around the actuator frequency increased. This also means the phase margin of the system decreases, and it would be more oscillatory for high-frequency inputs. However, this might be preferable since the performance and robustness issues are shifted to higher frequencies, where the robot usually does not operate.

D. Actuator dynamics compensation filter

As illustrated in Fig. 8, in case the actuator had no dynamics at all, the velocity compensation would be perfect and both performance and robustness would be ideal. Although such situation is not realistic, it brings important insights on how to improve the velocity compensation robustness. For instance, a lead compensator for the velocity compensation feedforward command can be applied. Differently than the notch filter, this compensator, or filter, would aim at minimizing the effects of the actuator dynamics in the feedforward path only. By applying a filter with twice the natural frequency of the actuator ω_a, and complex zeros around ω_a, an improved response is obtained and shown in solid green in Fig. 10. As we can see, such filtering in the feedforward path does not suffer from the waterbed effect, and an attenuation of the sensitivity is achieved in low and middle frequencies without compromising the sensitivity peak.

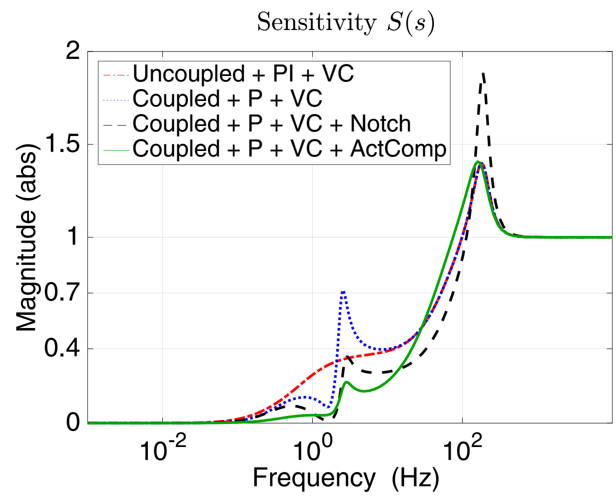

Fig. 10: Sensitivity function for the closed-loop force dynamics with different controllers. In dot-dashed red we show the uncoupled case using a PI feedback controller together with a velocity compensation (VC) feedforward. This uncoupled sensitivity does not present a dent at middle frequencies (around 2 Hz). On the other hand, in dotted blue we show the sensitivity for the coupled system with a P controller and the same VC feedforward. In this case a dent appears because of the human/robot coupling. In dashed black is a solution with a notch filter, which reduces the sensitivity in middle frequencies but increases it at high frequencies. Finally, in solid green we show the sensitivity when a lead filter to perform an actuator dynamics compensation (ActComp) is added to the feedforward path.

IV. Conclusions and Future Work

Because of a natural velocity feedback, intrinsic to the physics of force transmission, the dynamics of the robot actuator force depends not only on the actuator itself but also on the load characteristics. For a wearable robot, this is particularly relevant since the attachment with the user introduces important features into the load dynamics. The most critical one is a resonance/antiresonance at the natural frequency of the attachment.

In terms of force control robustness, the human/robot coupling significantly increases the sensitivity of the closed-loop system at low frequencies. This tends to make the force control more challenging at these frequencies, which are usually in the range of common human locomotion tasks such as walking and running. The exact frequency of this local sensitivity peak depends mainly on the attachment stiffness, and on the human characteristics, such as inertia, stiffness, and damping. To minimize this intrinsic coupling effect on the system sensitivity, we proposed two control solutions: a notch filter around the attachment resonance frequency, and/or a lead compensator on the feedforward path. Both solutions demonstrate potential to reduce the sensitivity magnitude to values comparable to uncoupled robots. Such lower sensitivity would lead, on its turn, to a better disturbance rejection and reference tracking for the closed-loop force controller.

Future work include the implementation and evaluation of such control solutions on a real robot, and a thorough analysis of the influence of human parameters such as joint impedance into the force control performance and stability. Ultimately, such algorithms shall be tested with human subjects.

ACKNOWLEDGEMENTS

This research has been supported by a Swiss National Science Foundation Professorship Award to Jonas Buchli and the EU Project BALANCE (Grant 601003 of the EU FP7 program).

REFERENCES

[1] N. Hogan, "Impedance control: An approach to manipulation: Part II – Implementation," *ASME, Transactions, Journal of Dynamic Systems, Measurement, and Control*, vol. 107, pp. 8–16, 1985.

[2] M. raibert and J. Craig, "Hybrid position/force control of manipulators," *ASME Journal of Dynamic Systems, Measurement, and Control*, vol. 107, pp. 126–133, 1981.

[3] O. Khatib, "A unified approach for motion and force control of robot manipulators: The operational space formulation," *IEEE Journal of Robotics and Automation*, vol. 3, no. 1, pp. 43–53, 1987.

[4] J. Pratt, C. Chew, A. Torres, P. Dilworth, and G. Pratt, "Virtual model control: An intuitive approach for bipedal locomotion," *The International Journal of Robotics Research*, vol. 20, no. 2, pp. 129–143, 2001.

[5] B. Armstrong-Hlouvry, P. Dupont, and C. C. D. Wit, "A survey of models, analysis tools and compensation methods for the control of machines with friction," *Automatica*, vol. 30, no. 7, pp. 1083 – 1138, 1994. [Online]. Available: http://www.sciencedirect.com/science/article/pii/0005109894902097

[6] F. Conrad and C. Jensen, "Design of hydraulic force control systems with state estimate feedback," in *IFAC 10th Triennial Congress*, Munich, Germany, 1987, pp. 307–31.

[7] T. Boaventura, M. Focchi, M. Frigerio, J. Buchli, C. Semini, G. Medrano-Cerda, and D. Caldwell, "On the role of load motion compensation in high-performance force control," in *IEEE/RSJ International Conference on Intelligent Robots and Systems (IROS)*, oct. 2012, pp. 4066 –4071.

[8] C. Flynn, A. Taberner, and P. Nielsen, "Mechanical characterisation of in vivo human skin using a 3d force-sensitive micro-robot and finite element analysis," *Biomechanics and Modeling in Mechanobiology*, vol. 10, no. 1, pp. 27–38, 2010. [Online]. Available: http://dx.doi.org/10.1007/s10237-010-0216-8

[9] K. Kong, J. Bae, and M. Tomizuka, "Control of rotary series elastic actuator for ideal force-mode actuation in human–robot interaction applications," *IEEE/ASME Transactions on Mechatronics*, vol. 14, no. 1, pp. 105–118, Feb 2009.

[10] G. Pratt and M. Williamson, "Series elastic actuators," in *IEEE International Conference on Intelligent Robots and Systems (IROS)*, 1995.

[11] N. Paine, S. Oh, and L. Sentis, "Design and control considerations for high-performance series elastic actuators," *IEEE/ASME Transactions on Mechatronics*, vol. 19, no. 3, pp. 1080–1091, June 2014.

[12] S. Dyke, B. Spencer Jr., P. Quast, and M. Sain, "Role of control-structure interaction in protective system design," *Journal of Engineering Mechanics, ASCE*, vol. 121 No.2, pp. 322–38, 1995.

[13] S. Pfeifer, R. Riener, and H. Vallery, "Knee stiffness estimation in physiological gait," in *Engineering in Medicine and Biology Society (EMBC), 2014 36th Annual International Conference of the IEEE*. IEEE, 2014, pp. 1607–1610.

[14] E. J. Rouse, L. J. Hargrove, E. J. Perreault, and T. A. Kuiken, "Estimation of human ankle impedance during walking using the perturberator robot," in *Biomedical Robotics and Biomechatronics (BioRob), 2012 4th IEEE RAS & EMBS International Conference on*. IEEE, 2012, pp. 373–378.

[15] H. Lee and N. Hogan, "Time-varying ankle mechanical impedance during human locomotion," 2014.

[16] R. Dhaouadi, K. Kubo, and M. Tobise, "Analysis and compensation of speed drive systems with torsional loads," in *Proceedings of the Power Conversion Conference*, 1993, pp. 271–277, yokohama.

[17] Y. Hori, H. Iseki, and K. Sugiura, "Basic consideration of vibration suppression and disturbance rejection control of multi-inertia system using sflac (state feedback and load acceleration control)," *IEEE Transactions on Industry Applications*, vol. 30, no. 4, pp. 889–896, 1994.

[18] T. Boaventura, C. Semini, J. Buchli, M. Frigerio, M. Focchi, and D. G. Caldwell, "Dynamic torque control of a hydraulic quadruped robot," in *IEEE International Conference in Robotics and Automation (ICRA)*, 2012, pp. 1889–1894.

[19] A. Herzog, L. Righetti, F. Grimminger, P. Pastor, and S. Schaal, "Momentum-based balance control for torque-controlled humanoids," *CoRR, vol. abs/1305.2042*, 2013.

[20] G. Franklin, *Feedback Control of Dynamic Systems*, 3rd ed., G. Franklin, J. Powell, and A. Emami-Naeini, Eds. Addison-Wesley Longman Publishing, Boston, 1993.

[21] D. E. Seborg, D. A. Mellichamp, T. F. Edgar, and F. J. Doyle III, *Process dynamics and control*. John Wiley & Sons, 2010.

[22] S. Skogestad and I. Postlethwaite, *Multivariable feedback control: analysis and design*. Wiley New York, 2007, vol. 2.

[23] S. Dormido and F. Morilla, "Tuning of pid controllers based on sensitivity margin specification," in *Control Conference, 2004. 5th Asian*, vol. 1. IEEE, 2004, pp. 486–491.

[24] V. Sule and V. Athani, "Directional sensitivity tradeoffs in multivariable feedback systems," *Automatica*, vol. 27, no. 5, pp. 869–872, 1991.